reactions

MDPI

Article

Thiol-Ene Click-Inspired Late-Stage Modification of Long-Chain Polyurethane Dendrimers

Dhruba P. Poudel and Richard T. Taylor *

Department of Chemistry and Biochemistry, Miami University, Oxford, OH 45056, USA; poudeld@miamioh.edu
* Correspondence: taylorrt@miamioh.edu

Abstract: The construction of well-defined polyurethane dendrimers is challenging due to the high reactivity of externally added or in situ formed isocyanates leading to the formation of side products. With a primary focus of dendrimer research being the interaction of the periphery and the core, we report the synthesis of a common polyurethane dendron, which allows for the late-stage variation of both the periphery and the core. The periphery can be varied simply by installing a clickable unit in the dendron and then attaching to the core and vice-versa. Thus, a common dendron allows for varying periphery and core in the final two steps. To accomplish this, a protecting group-free, one-pot multicomponent Curtius reaction was utilized to afford a robust and versatile AB_2 type polyurethane dendron employing commercially available simple molecules: 5-hydroxyisophthalic acid, 11-bromoundecanol, and 4-penten-1-ol. Subsequent late-stage modifications of either dendrons or dendrimers via a thiol-ene click reaction gave surface-functionalized alternating aromatic-aliphatic polyurethane homodendrimers to generation-three (G3). The dendrons and the dendrimers were characterized by NMR, mass spectrometry, and FT-IR analysis. A bifunctional AB_2 type dendritic monomer demonstrated this approach's versatility that can either undergo a thiol-ene click or attachment to the core. This approach enables the incorporation of functionalities at the periphery and the core that may not withstand the dendrimer growth for the synthesis of polyurethane dendrimers and other dendritic macromolecules.

Keywords: polyurethane dendrimers; late-stage modification; thiol-ene click reaction; dendrons

Citation: Poudel, D.P.; Taylor, R.T. Thiol-Ene Click-Inspired Late-Stage Modification of Long-Chain Polyurethane Dendrimers. *Reactions* **2022**, *3*, 12–29. https://doi.org/10.3390/reactions3010002

Academic Editors: Lelia Cosimbescu and Dmitry Yu. Murzin

Received: 2 December 2021
Accepted: 19 December 2021
Published: 22 December 2021

Publisher's Note: MDPI stays neutral with regard to jurisdictional claims in published maps and institutional affiliations.

1. Introduction

Dendrimers are highly branched, multivalent, star-shaped polymeric macromolecules [1–4]. These monodispersed dendritic polymers exhibit wide applications in the field of catalysis, sensing, molecular electronics, photonics, fluorescence, and therapeutics [5–20]. After Tomalia's first report on poly(amidoamine) (PAMAM) dendrimers in 1985, ref [21] many research groups have reported the synthesis of dendritic macromolecules using ether, ester, carbosilane, amide, and alkyne linkages [21–33]. Few have reported the synthesis of dendrimers having a urethane linkage indicating that polyurethane dendrimers [34] have not been studied extensively. The construction of a well-defined architecture of a polyurethane dendrimer is challenging due to isocyanates' high reactivity [35]. Pioneering works published simultaneously in 1993 by two research groups established the synthetic routes to polyurethane dendrimers. The first route described by Spindler and Fréchet [36,37] used isocyanate chemistry. In contrast, the second route described by Kumar and Ramakrishnan [38] employed an isocyanate-free approach to synthesize polyurethane dendrimers. Following these pioneering works, a few more dendritic polyurethanes have been reported [39–46]. More recently, Nasar and coworkers have reported the synthesis of hyperbranched polyurethanes and polyurethane dendrimers based on blocked isocyanate chemistry [47–52].

Dendrimers have been synthesized via well-established convergent and divergent methods. The convergent method involves a small number of reactions per molecule during the coupling and activation of dendrons [53]. This provides greater structural control

than with divergent protocol. First reported by Hawker and Fréchet for the synthesis of poly(phenyl benzyl ether) dendrimers, ref [54] the convergent method ensures the precise placement of functional groups throughout the dendritic structure that enables the synthesis of functional macromolecules. Though several dendrimers are reported recently employing the convergent method of synthesis, refs [21,24,54–72] there are very few reports on polyurethane dendrimers using this method [40,73–75].

The thiol-ene click reaction, one of the standard click reactions, is most frequently photoinduced and proceeds with quantitative yield with a rapid reaction rate. It is insensitive to moisture and yields a single stereoselective product [76,77]. For this reason, thiol-ene click reactions have been widely exploited for the synthesis, functionalization, and postmodification/surface modification of dendrimers for the formation of cross-linkages in hyperbranched macromolecules [50,77–107]. This powerful tool has seen little application in the field of polyurethane chemistry. There are only two reports of the thiol-ene click reaction employed for the synthesis of hyperbranched aliphatic polyurethanes [108,109].

Our group reported the convergent synthesis of polyurethane dendrimers having dodecyl end groups, using a protection–deprotection strategy two decades ago [110,111]. Herein, we report on a fast, efficient, and protecting-group-free approach to synthesize polyurethane dendrimers to the third generation (G3) using the convergent method. Using this approach, the periphery can be varied simply by installing a clickable unit in the dendron followed by its attachment to the core, and the core can be varied in the final step before the dendron's attachment. Thus, a common dendron allows for varying the periphery and the core in just the final two steps. Commercially available 5-hydroxyisophthalic acid, 4-penten-ol, and 11-bromoundecanol were required to furnish an AB_2 type common polyurethane dendron. The subsequent late-stage modification of either dendron or dendrimer via the thiol-ene click reaction gave surface-functionalized, alternating aliphatic-aromatic polyurethane homodendrimers. As shown in Scheme 1, an AB_2 type dendritic monomer can either undergo a thiol-ene click followed by attachment to the core or vice-versa to yield post-modified dendrimers. Previously, we demonstrated this strategy in detail concerning generation one (G1) dendrimers [112]. In this work, we extend our previous approach to synthesize the polyurethane dendrimers to G3.

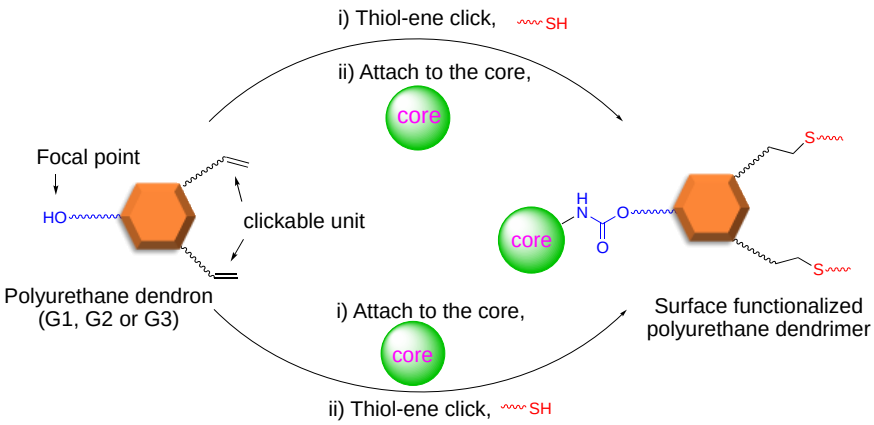

Scheme 1. General representation of synthetic strategy.

2. Results and Discussion

Synthesis of linking agent and core. Commercially available 5-hydroxyisophtalic acid **1** was used as a building block to synthesize the generation one dendritic wedge $\mathbf{(G1W)_{ene}}$ (or simply a dendron), ref [112] whereas unprotected 5-hydroxy-1,3-diacyldiazide **4** was utilized as a linking group or branching point to afford the G2 or G3 dendron (Scheme 2). Linking group **4**, a white amorphous solid was synthesized in a three-step sequence starting from **1** with an overall yield 79%, where **1** was esterified using methanol followed by nucleophilic substitution with hydrazine and treatment with sodium nitrite un-

der acidic medium. To synthesize a trifunctional core **6**, 1,3,5-benzenetricarbonyltrichloride was treated with sodium azide forming acyl azide at room temperature, which upon heating underwent a Curtius rearrangement affording 1,3,5-triisocyanatobenzene **6** [113] as needle-shaped crystals on heating (87% yield).

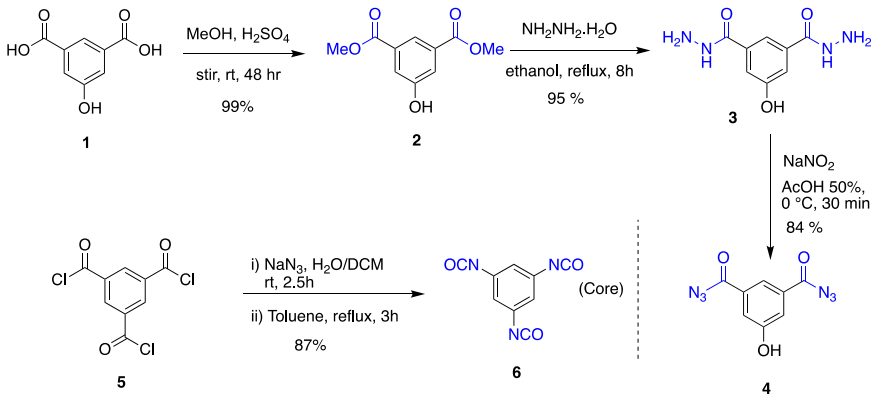

Scheme 2. Synthesis of linking group **4** and core **6**.

Synthesis of G1 dendrimer. With a core and a building block in hand, a series of polyurethane dendrimers starting from G1 were prepared using 4-penten-1-ol and 11-bromoundecanol as the peripheral and spacer groups, respectively. As previously reported, the G1 dendron required for this operation was prepared from **1** in two steps (Scheme 3) [112]. It's noteworthy that the diurethane **7** can also be used as a dendron, but the reactivity is lower than that of alcoholic OH. Also, the installation of the undecyl group improves the solubility even for higher generation dendrons and dendrimers.

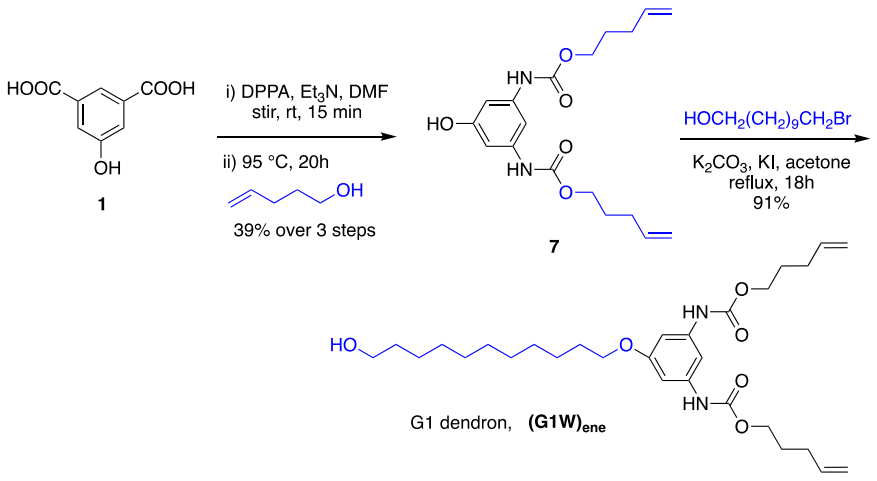

Scheme 3. Synthesis of G1 dendron using one-pot multicomponent Curtius reaction.

The advantages of this strategy of dendron formation are that the reaction proceeds smoothly in one pot without the need of separating the intermediate isocyanate, and the byproduct, diphenylphosphoric acid, can be separated from the desired product simply by using flash chromatography. Our group had already succeeded in preparing polyurethane dendrimers employing a variation of this method [111]. However, the current approach does not require any protection at the focal point of the dendron, which significantly reduces the synthetic steps. Moreover, the current strategy allows one to synthesize the dendron on a multigram scale.

Convergent synthesis permits the modification of dendrons at the focal point. Moreover, this approach allows the post derivatization of peripheral groups without disturbing

the core and repeating units' functionality [53] Exploiting this theme, we previously demonstrated our late-stage modification strategy's versatility by synthesizing G1 dendrimers using thiol-ene click chemistry [76]. As shown in Scheme 4, dendrimer **G1D** can be constructed via two different routes—(i) click and attach approach (premodification) and (ii) attach and click approach (postmodification)—starting from dendron **(G1W)$_{ene}$**. Our previous method of dendron formation allows us to change both the periphery and core in just two steps. The peripheral groups can be changed by installing a different clickable unit, whereas a different core can be used during the dendron's attachment to it.

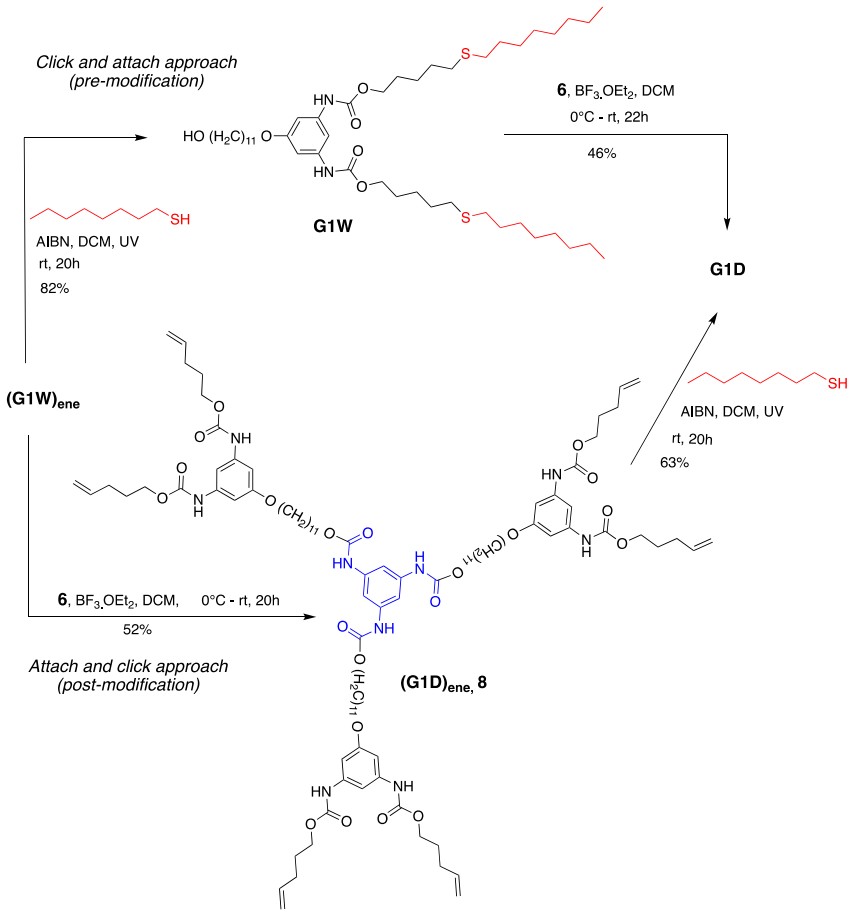

Scheme 4. Late-stage modification of G1 dendron and dendrimer using the thiol-ene click reaction.

Synthesis of G2 and G3 dendrimers. As depicted in Scheme 5, growth of higher generation dendritic wedges commenced with coupling **1** with G1 dendron **(G1W)$_{ene}$** under the Curtius reaction conditions using diphenylphosphoryl azide (DPPA) as an azide source and Et_3N as a base, which gave G2 phenolic dendron **9**. However, the yield of this reaction was significantly lower than that of **7** (Scheme 3). Such a low yield could be attributed partially to the lower reactivity of the larger attacking nucleophile **(G1W)$_{ene}$** compared with 11-bromoundecanol and partially to the side product, diphenyl phosphoric acid produced from DPPA during the reaction. To overcome these difficulties, we synthesized **4** as the linking group with a free OH group on it (Scheme 2), which undergoes the Curtius reaction without any catalyst to form **9** with a good yield (64%).

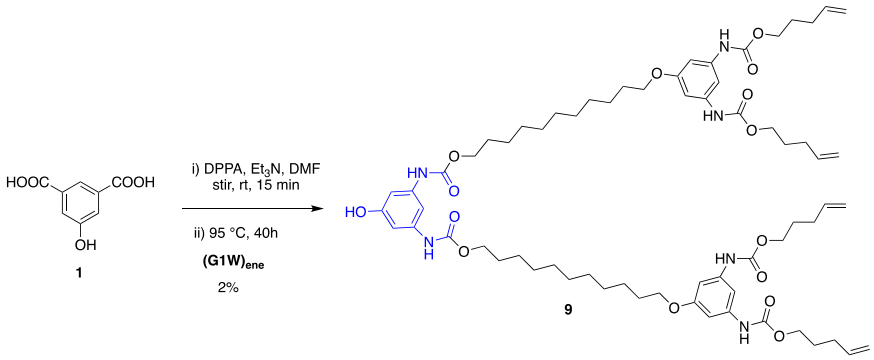

Scheme 5. Synthesis of G2 dendron from 5-hydroxyisophthalic acid.

Having optimized the proper reaction conditions, we started the coupling of the G1 dendron **(G1W)$_{ene}$** with the linking agent **4**. The reaction preceded smoothly on heating at 95 °C under the Curtius reaction conditions in DMF to afford G2 phenolic urethane **9**. G2 dendron **(G2W)$_{ene}$** with the pentene periphery was produced when **9** was heated with 11-bromoundecanol, the spacer group used in this study. In situ formed isocyanate during the Curtius rearrangement could be activated by adding a Lewis acid such as $BF_3.OEt_2$ as a catalyst, however, did not accelerate the formation of the product because of the solvent (DMF) coordinated with the catalyst. Moreover, a base such as Et_3N as a catalyst would render the unprotected phenolic OH more nucleophilic, leading to the phenolic attack on in situ formed isocyanate, thereby increasing the side products' yield. Therefore, we carried out this reaction without any catalyst, and better results were obtained over a longer time. The thiol-ene functionalization of the peripheral alkene moieties with 1-octanethiol in the presence of 2,2′-azobis(2-methylpropionitrile) (AIBN) free-radical initiator under a UV light formed the G2 dendron, **G2W,** containing the thioether functionality in the end groups. In its final step, the periphery-modified **G2W** was attached to the trifunctional core **6** in the presence of the Lewis acid catalyst $BF_3.OEt_2$ to afford the generation-two dendrimer, **G2D,** as a highly viscous, transparent gel. Figure 1 shows the FT-IR monitored-progress of the $BF_3.OEt_2$-catalyzed reaction involving the attachment of the dendron to the core.

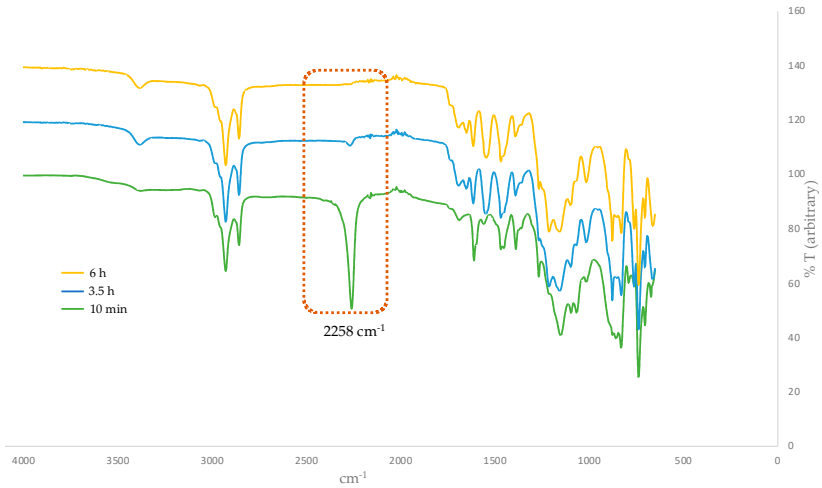

Figure 1. Progress of $BF_3.OEt_2$-catalyzed reaction involving the attachment of dendron to the core monitored by FT-IR spectroscopy. The isocyanate N=C=O stretch at 2258 cm^{-1} disappears over time.

The iteration of the Curtius reaction followed by the undecyl group attachment (steps i and ii, Scheme 6) to the phenolic wedge **10** produced the generation-three dendron **(G3W)$_{ene}$** starting from the generation-two dendritic wedge **(G2W)$_{ene}$** and linking group **4**. Peripheral pentene moieties of this G3 dendron were subjected to the thiol-ene click

conditions as in the G1 and G2 steps to form a modified G3 dendron, **G3W**, which was then attached to the trifunctional core **6** to generate the G3 dendrimer, **G3D**. Figure 2 (and Figures S1–S5) shows the structures of G1–G3 polyurethane dendrimers synthesized in this work.

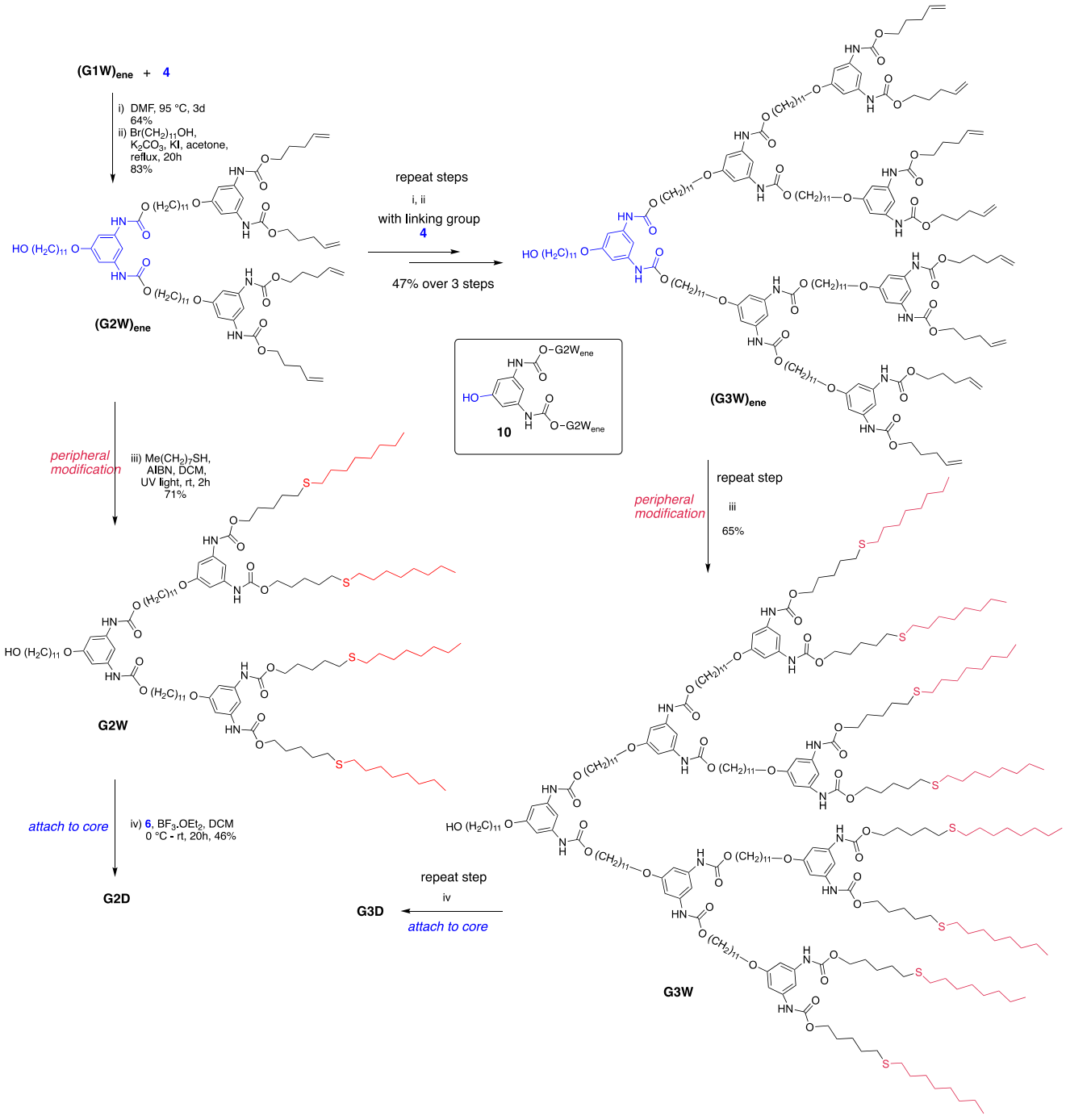

Scheme 6. Synthesis showing the growth of G2–G3 dendrons and dendrimer.

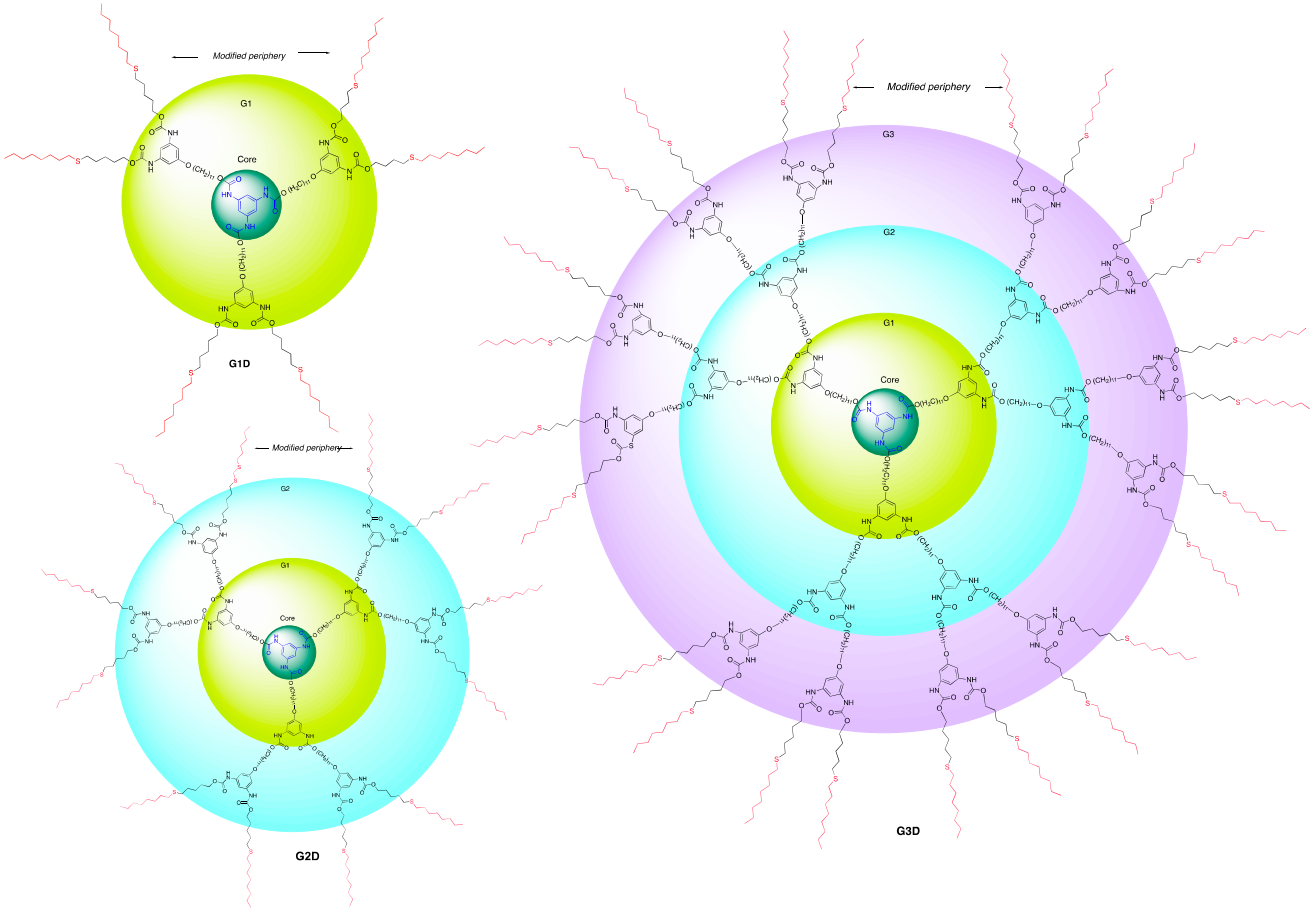

Figure 2. Structure of synthesized G1, G2, and G3 dendrimers showing modified periphery.

Our strategy allows for the growth of a new generation dendron in every two steps, thereby furnishing G3 dendron (with an alkene periphery in this case) only over six steps. The first of the two steps involve the Curtius reaction that generates a urethane linkage via the nucleophilic attack of alcohol on the in situ formed isocyanate (obtained from the internal rearrangement of acyl azide), and the second step involves the attachment of the undecyl group as a tail. Both reactions do not require protection—deprotection and the products can be purified easily using silica gel chromatography. The advantage of using a clickable periphery is that these groups remain unreactive during the growth of the dendron.

As shown in Scheme 6, we employed the click and attach approach to synthesize the G2 and G3 dendrimers. The reasoning behind this can be explained in terms of yield and the complexity of the reaction. Our study showed that the click-then-attach approach proceeds with better yields than that of the attach-then-click approach (Scheme 4). The attachment of the dendron to a trifunctional core involves the same number of reactions per molecule in both approaches; however, the end group modification by the thiol-ene click reactions during the attach-then-click approach requires a large number of reactions per molecule to undergo completion. Such transformations suffer from the same complications as the divergent synthesis, as the multiplicity of the end groups increases with the higher generation resulting in incomplete or side reactions or even degradation of branches, which burdens the purification of the dendrimer.

Characterization of dendritic structures. The thiol-ene click modified polyurethane dendrimers **G1D-G3D** were first characterized by one-dimensional multinuclear (^{1}H and ^{13}C) as well as two-dimensional (2D) homonuclear and heteronuclear NMR spectroscopy (Figures S6–S30). As shown in the ^{1}H NMR spectra (Figures 3, S18, S19 and S27), between

8.0–0.0 ppm, the peaks of protons assigned to **G1D-G3D** remain unchanged, indicating the identical structures of the dendrimers. However, these peaks became broader with increasing generations, possibly due to the tumbling effect associated with viscosity ongoing from the first to the third-generation dendrimer. In the stacked ^{1}H NMR of G2 dendrimeric structures (Figure 3a), the peaks at ~5.9–5.0 ppm assigned to the terminal alkenes disappeared, ultimately indicating that the thiol-ene reaction went successfully to completion. This formation of new peaks—a quartet at ~2.5 ppm (formed due to the overlapping of two different triplets) and a triplet at ~0.9 ppm assigned to -SCH_2- and the terminal -CH_3 groups, respectively—further supports the completion of the thiol-ene reaction. The attachment of the dendrons, **G1W-G3W**, to the trifunctional core was evidenced by the appearance of a new ^{1}H peak at the aromatic region (Figure 3a purple spectrum and Figure 3b). The expanded region of Figure 3b shows the aromatic protons' peaks of **G3D** where a more shielded broad peak at ~6.8 ppm is assigned to both the NHs and aromatic protons ortho to aryl ethers. In contrast, the most deshielded peak at ~7.3 ppm accounts for the aromatic protons of the core. The G1-G3 dendrimers were also characterized by two-dimensional homonuclear and heteronuclear NMR spectroscopy. Figure 3c shows an aromatic region of two-dimensional heteronuclear single quantum coherence (HSQC) spectroscopy of **G3D** where the more downfield peak (~7.25 ppm, 110 ppm) corresponds to the aromatic proton of the trifunctional core.

Mass spectrometric investigation of the polyurethane dendrimers, **G1D-G3D**, was performed by matrix-assisted laser desorption/ionization time-of-flight mass spectrometry (MALDI-TOF-MS), which supported the structure of these dendrimers. In the MALDI-TOF-MS spectrum (Figures S38–S45), the peak of m/z = 2633.70 detected was consistent with the theoretical mass of [**G1D** + H]$^+$ ion (m/z = 2632.70 Da). The peak at m/z = 6129.89 detected in the MALDI-TOF-MS spectrum (Figure S41) corresponded to the [**G2D** + Na]$^+$ ion (theoretical m/z = 6125.94 Da). For the polyurethane dendrimer, **G3D** (theoretical mass = 13,043.46 Da), the MALDI-TOF-MS spectrum provided unsatisfactory mass data, possibly because the dendrimer absorbed the laser wavelength (355 nm) used in the instrument, subsequently fragmenting the compound before it gives the [**G3D**]$^+$ signal. (As shown in the Figure S54, the **G3D** has broad absorption from 280–360 nm with an emission-maxima at 382 nm, Figure S55). High resolution mass spectrum of linking group **4** is shown in Figure S37.

To further determine the structure of **G1D-G3D**, we also employed a two-dimensional (2-D) diffusion-ordered spectroscopy (DOSY). The observation of a distinct spectral band in the DOSY spectrum (Figures S31–S36) of the dendrimers implied the existence of **G1D**, **G2D**, or **G3D**. Moreover, a gradual decrease in the diffusion coefficient (D) observed—4.47 $\times$ 10^{-10} (**G1D**), 1.86 $\times$ 10^{-10} (**G2D**), and 1.38 $\times$ 10^{-10} (**G3D**)—in the spectrum provided further evidence of a progressive increase in the size of the dendrimers with increasing generations.

Investigation of G2–G3 dendrons and dendrimers using Fourier-transform infrared spectroscopy are presented in Figures S46–S53.

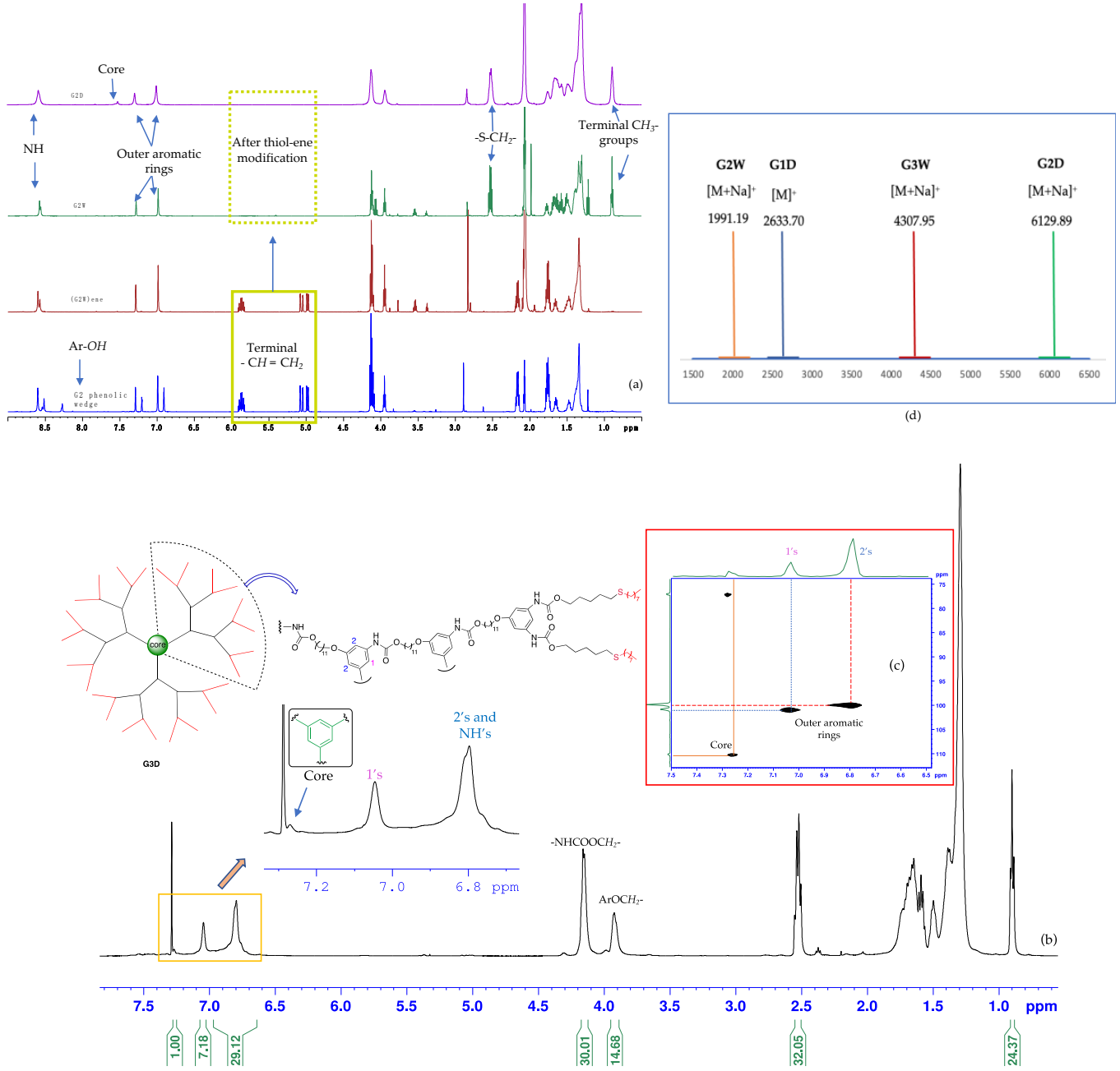

Figure 3. (**a**) Representative ^{1}H NMR spectra (stacked) showing the G2 phenolic wedge **9**, **(G2W)$_{ene}$**, **G2W**, and **G2D,** respectively, from bottom to top, (**b**) ^{1}H NMR spectrum of **G3D**: integrals in full spectrum show the one-third portion of this C_3 symmetric molecule, whereas the expanded region depicts aromatic protons of both core and peripheral groups, (**c**) a portion of HSQC of **G3D** showing heteronuclear ^{1}H-^{13}C coupling at aromatic region, and (**d**) MALDI-TOF spectra of G1-G3 dendrons and dendrimers (NMR spectra were recorded in 500 MHz spectrometer at 298 K using CD_3COCD_3 as deuterated solvent).

3. Conclusions

In summary, we demonstrated a thiol-ene click-inspired, protecting group-free approach towards the convergent synthesis of polyurethane dendrimers. The one-pot multicomponent Curtius reaction followed by a spacer group's attachment gave a new generation common dendron in every two-step, which allowed for the late-stage modification of both the periphery and the core. Thioether surface functionalized polyurethane G1 dendrimers were synthesized via both the click-then-attach and the attach-then-click approaches using

a trifunctional core. Higher generation dendrimers, **G2D** and **G3D**, were synthesized employing the click-then-attach strategy to minimize the incomplete reactions and possible degradations at the periphery that could be associated with the attach-then-click approach. Access to this type of strategy will contribute to a concise and efficient synthesis of not only the polyurethane dendrimers but also other dendritic macromolecules. Our ongoing research also involves the synthesis and characterization of dendrimers with alkyne moieties, which undergo late-stage modification using azide-alkyne click chemistry.

4. Experimental Section

General information. Starting materials were used as obtained from commercial sources: Sigma Aldrich (NaN_3, AIBN, 1-octadecanethiol, triethylamine), TCI (4-penten-1-ol, 1-bromoundecanol, benzene-1,3,5-trcicarbonyltrichloride, 1-octanethiol, $BF_3.OEt_2$), and Alfa Aesar (5-hydroxyisophthalic acid, diphenylphosphoryl azide (DPPA)), whereas anhydrous solvents were used in the dendrimer synthesis, DMF (Acros Organics), DCM (Fischer Scientific) and acetone (Acros Organics) were used as received, and reagent toluene was used without distillation. The Curtius reaction was set in a Carousel reactor, and all other reactions were performed using the classical batch process using an oil bath (if heat was needed). A UV lamp from the American Ultraviolet Company (model: PC-100S; 120 V, 60 Hz, 5 Amp; S/N: 9902L3669) was used to carry out the thiol-ene click reaction. Melting points were determined using a Thermo Scientific MelTemp 3.0 instrument.

^{1}H, ^{13}C, and 2D NMR spectra were recorded with a Bruker Advance 500 MHz NMR instrument at 298 K. NMR spectra were recorded using either acetone-d_6 or $CDCl_3$ as a deuterated solvent, and, accordingly, the solvent residual peaks were obtained at δ 2.05 ppm (qn) and δ 7.26 ppm (s), respectively, in ^{1}H NMR. In ^{13}C NMR, the solvent residual peaks were recorded at δ 206.68 ppm (s) and δ 29.92 ppm (septet) for acetone-d_6 and δ 77.23 ppm (s) for $CDCl_3$. Coupling constants (*J*) are given in hertz (Hz), whereas chemical shifts are given in δ scale (ppm). Moreover, the multiplicities are indicated as—s (singlet), d (doublet), t (triplet), q (quartet), qn (quintet), or m (multiplet). The IR spectra were obtained from the PerkinElmer Spectrum One FT-IR Spectrometer.

The HRMS spectra of small molecules, including dendrons, were obtained from the FTMS plus CESI mass spectrometer using DCM as a solvent. The MALDI of larger molecules was recorded with a Bruker Autoflex 3 instrument using dithranol and ferulic acid as the matrix in positive ion mode.

The purification of compounds was carried out using flash chromatography with irregular silica of 40–60 μm, 60 Å. Small scale purification was achieved using auto column flash cartridges packed with 12 g or 40 g silica of 40–75 μm, 60 Å (obtained from Sorbtech and Supelco Technologies). The flow rate was 10 mL/min–30 mL/min. The mobile phase used in these separations was ethyl acetate, hexane, DCM, or a mixture of these solvents.

General procedure of the Curtius reaction. Method 1. An oven-dried carousel tube was charged with 5-hydroxyisophthalic acid **1** and a magnetic stir bar. After degassing and backfilling the tube with nitrogen, anhydrous DMF was added. The compound was dissolved completely, followed by the slow addition of Et_3N and the dropwise addition of DPPA under stirring at an ambient temperature. After stirring the solution for 15 min, the dendron was added, and the tube was transferred to a carousel reactor maintained at 95 °C. The reaction was monitored with TLC. After 40 h, the solution was cooled to room temperature, diluted with 20 volumes of water, and extracted with EtOAc (three times). The combined organic layers were washed with water (five times) and brine (once), concentrated under reduced pressure, and purified by flash chromatography.

Method 2. An oven-dried carousel tube was charged with 5-hydroxy-1,3-dicarbonyl diazide **4** and the dendron. After degassing and backfilling the tube with nitrogen, anhydrous DMF was added, and then the solution was transferred to the carousel reactor and maintained at 95 °C. The reaction was monitored with TLC. After 72 h, the work-up was performed similarly to method 1.

General procedure of thiol-ene click reaction. The dendron with an alkene periphery was dissolved in anhydrous DCM in a glass vial. 1-Octanethiol (1.1 eq/double bond) and AIBN (0.1 eq/double bond, as a free-radical initiator) were added to the solution. The vial was then capped and placed under a broad-spectrum UV lamp under stirring at an ambient temperature. After 2 h, the solvent was evaporated, and the crude was purified by flash chromatography.

General procedure of attachment of dendron to the core. An oven-dried RB flask was charged with 1,3,5-triisocyanatobenzene and a magnetic stir bar. After degassing and backfilling the flask with nitrogen, anhydrous DCM was added via syringe. The flask was then placed under an ice bath and three drops of $BF_3.OEt_2$ were added. After stirring 10 min, a solution of dendron in anhydrous DCM was added dropwise, and stirring was continued for 10 min. The ice bath was removed, and the stirring was continued for 20 h. The progress of the reaction was monitored using FT-IR observing the isocyanate peak at ~2200 cm^{-1}. When the peak disappeared, the stirring was stopped, the solvent was evaporated, and the crude was purified by flash chromatography.

Synthetic procedure of compounds from **7** to **G1D** has been reported previously [112].

5-Hydroxy-1,3-benznedicarbonyl diazide **4**. Dimethyl-5-hydroxyisophthalte **2** (10 g, 47.6 mmol, 1.0 eq) was dissolved in ethanol (100 mL) in a 250 mL RB flask containing a magnetic stir bar. Hydrazine hydrate (14.65 mL, 51%, 142.8 mmol, 5.0 eq) was added, and the mixture was refluxed. The progress of the reaction was checked with TLC (1:1 EtOAc/hexane). After 8 h, that white solid that formed was filtered, washed with cold ethanol, and dried under a vacuum overnight to get the white powder as the product **3** (9.54 g, 45.4 mmol, 95% yield, m.p. 257 °C). It was carried to the next step without further purification.

5-Hydroxy-1,3-benzenedicarboxylic acid-1,3-dihydrazide **3** (9.54 g, 45.43 mmol, 1.0 eq) was dissolved in 50% *v*/*v* acetic acid (120 mL) in a 250 mL RB flask containing a magnetic stir bar. The solution was placed in an ice-bath, and $NaNO_2$ (9.40 g in 90 mL MQ water, 136.29 mmol, 3.0 eq) was added dropwise at 0 °C. Stirring was continued for 30 min at the same temperature. The white solid formed during the reaction was filtered, washed with cold water, and dried under a vacuum to obtain compound **4** as the product (8.86 g, 38.16 mmol, 84% yield). It was pure enough for further reactions. TLC (35% EtOAc in hexane): R_f 0.46. ^{1}H NMR (500 MHz, CD_3COCD_3): δ 9.42 (s, 1H, OH), 8.05 (t, *J* = 1.43 Hz, 1H), 7.72 (d, *J* = 1.45 Hz, 2H). ^{13}C NMR (126 MHz, CD_3COCD_3): δ 171.0, 158.2, 132.7, 121.0, 120.8. HRMS (ESI-LTQ-Orbitrap): *m*/*z* calculated for $C_8H_3N_6O_3^-$ [M-H]$^-$ 231.0272; found 231.0270.

Generation-two phenolic wedge **9**. The general procedure of the Curtius reaction (method 1) was employed using 5-hydroxyisophthalic acid **1** (66 mg, 0.362 mmol, 1.0 eq), anhydrous DMF (08 mL), Et_3N (106 µL, 0.760 mmol, 2.1 eq), DPPA (165 µL, 0.760 mmol, 2.1 eq), and **(G1W)$_{ene}$** (375.2 mg, 0.724 mmol, 2.0 eq) to obtain a transparent viscous oil as product **9** (22 mg, 0.018 mmol, 5%) after purification (40% EtOAc/hexane as mobile phase).

The general procedure of the Curtius reaction (method 2) was employed using 5-hydroxy-1,3-benzenedicarbonyl diazide **4** (579.3 mg, 2.500 mmol, 1.0 eq), **(G1W)$_{ene}$** (1941.5 mg, 3.743 mmol, 1.5 eq), and DMF (8 mL) to obtain a transparent, viscous oil as product **9** (1436.8 mg, 1.19 mmol, 64%) after purification (40% EtOAc/hexane as mobile phase). TLC (40% EtOAc in hexane): R_f 0.44. ^{1}H NMR (500 MHz, CD_3COCD_3): δ 8.58 (t, 6H, -NH-), 8.28 (s, 1H, OH), 7.29 (s, 2H), 7.20 (q, *J* = 1.9 Hz, 1H), 6.99 (s, 4H), 6.90 (s, 2H), 5.89–5.84 (m, 4H), 5.07–4.97 (qd, *J* = 17.1, 11.1, 9.2, 1.7 Hz, 8H), 4.12 (t, 12H), 3.95 (t, *J* = 6.5 Hz 4H), 2.19–2.14 (m, 8H), 1.78–1.74 (m, 12H), 1.67–1.64 (m, 4H), 1.49–1.46 (m, 4H), 1.43–1.29 (m, 24H). ^{13}C NMR (126 MHz, CD_3COCD_3): δ 160.1, 158.1, 153.54, 153.51, 153.46, 140.7, 140.6, 137.9, 114.6, 114.5, 100.7, 100.0, 99.9, 99.2, 67.6, 64.3, 63.7, 63.6, 61.6, 29.8, 28.1, 25.9, 25.7. MALDI-TOF-MS (*dithranol* as matrix): *m*/*z* calculated for $C_{66}H_{96}N_6O_{15}Na$ [M + Na]$^+$ 1235.68; found [M + Na]$^+$ 1235.67.

Generation two dendron, **(G2W)$_{ene}$**. An oven-dried 50 mL RB flask was charged with 11-bromoundecanol (156.0 mg, 0.620 mmol, 1.5 eq), K_2CO_3 (285.4 mg, 2.065 mmol, 5.0 eq), KI (13.8 mg, 0.083 mmol, 0.2 eq), anhydrous acetone (5 mL), and a magnetic stir bar.

After degassing and filling the flask with nitrogen, **9** (501.1 mg, 0.413 mmol, 1.0 eq) in 1.5 mL anhydrous acetone was transferred into the flask via syringe. The reaction mixture was set to reflux under nitrogen. The progress of the reaction was checked with TLC (3:2 hexane/EtOAc). After 20 h, the solvent was evaporated, and the crude was extracted with EtOAc, washed with brine, dried with anhydrous $MgSO_4$, concentrated, and finally purified by flash chromatography using 40% EtOAc in hexane as the mobile phase to obtain a slightly yellow, viscous oil as the product (475.5 mg, 0.344 mmol, 83% yield). TLC (40% EtOAc in hexane): R_f 0.41. ^{1}H NMR (500 MHz, CD_3COCD_3): δ 8.58 (d, 6H, NH), 7.29 (s, 3H), 6.99 (s, 6H), 5.91–5.82 (m, 4H), 5.08–4.97 (dq, *J* = 17.1, 10.2, 1.5 Hz, 8H), 4.12 (q, *J* = 6.7 Hz, 12H, overlapped triplet), 3.95 (t, *J* = 6.5 Hz, 6H), 3.55 (q, *J* = 18.4, 5.7 Hz, 2H), 3.40 (t, *J* = 5.3 Hz 1H, OH), 2.19–1.80 (m, *J* = 7.2 Hz, 8H), 1.80–1.73 (m, 16H), 1.67–1.63 (m, *J* = 14.3 Hz, 4H), 1.53–1.29 (m, 53H). ^{13}C NMR (126 MHz, CD_3COCD_3): δ 160.1, 153.6, 153.5, 140.7, 140.6, 137.9, 114.6, 100.7, 99.2, 67.7, 64.4, 63.7, 61.6, 32.9, 29.8, 281., 25.9, 25.8, 25.7. MALDI-TOF-MS (*dithranol* as matrix): *m/z* calculated for $C_{77}H_{118}N_6O_{16}Na$ $[M + Na]^+$ 1405.85; found 1405.99.

Surface functionalized generation-two dendron, **G2W**. The general procedure of the thiol-ene click reaction was employed using **(G2W)$_{ene}$** (101 mg, 0.073 mmol, 1.0 eq), anhydrous DCM (0.4 mL), 1-octanethiol (112 µL, 0.584 mmol, 4.0 eq), and AIBN (5 mg, 0.029 mmol, 0.4 eq) to obtain a highly viscous, transparent oil as the product (123.9 mg, 0.063 mmol, 86% yield) after purification (40% EtOAc/hexane as mobile phase). TLC (30% EtOAc in hexane): R_f 0.41. ^{1}H NMR (500 MHz, CD_3COCD_3): δ 8.58 (d, 6H, NH), 7.28 (s, 3H), 6.99 (s, 6H), 4.12 (qn, *J* = 6.5 Hz, 12H, overlapped triplet), 3.95 (t, *J* = 6.5 Hz, 6H), 3.55 (q, *J* = 18.4, 5.5 Hz, 2H), 3.39 (t, 1H, *J* = 5.3 Hz, OH), 2.53 (q, *J* = 7.5 Hz, 16H), 1.77 (qn, *J* = 14.4, 6H), 1.72–1.25 (m, 136H), 0.89 (t, *J* = 6.9 Hz, 12H). ^{13}C NMR (126 MHz, CD_3COCD_3): δ 160.1, 153.60, 153.57, 160.66, 140.64, 100.8, 99.2, 67.6, 64.4, 64.2, 61.6, 59.7, 32.9, 31.7, 31.6, 31.4, 25.9, 25.8, 25.7, 25.0, 22.4, 13.6, 13.5. MALDI-TOF-MS (*dithranol* as matrix): *m/z* calculated for $C_{109}H_{190}N_6O_{16}S_4Na$ $[M + Na]^+$ 1990.30, MW 1991.97; found 1991.19.

Generation-two dendrimer, **G2D**. The general procedure of the attachment of the dendron to the core was employed using 1,3,5-triisocyanatobenzene **6** (7.3 mg, 0.036 mmol, 1.0 eq), **G2W** (233.9 mg, 0.119 mmol, 3.3 eq), $BF_3.OEt_2$ (three drops), and anhydrous DCM (1.5 mL) to obtain a highly viscous, transparent oil as the product (101.3 mg, 0.017 mmol, 46% yield) after purification (30% EtOAc/hexane as mobile phase). TLC (30% EtOAc in hexane): R_f 0.56. ^{1}H NMR (500 MHz, CD_3COCD_3): δ 8.58 (s, 21H), 7.53 (s, 3H), 7.29 (s, 9H), 6.99 (s, 18H), 4.13 (s, 42H), 3.94 (s, 18H), 2.52 (d, *J* = 6.8 Hz, 48H), 1.76–1.31 (m, 378H), 0.90 (s, 36H). ^{13}C NMR (126 MHz, $CDCl_3$): δ 160.3, 153.5, 139.6, 139.5, 99.1, 68.1, 65.4, 65.2, 32.2, 32.0, 31.8, 29.7, 29.5, 29.4, 29.3, 29.2, 29.1, 29.0, 28.9, 28.6, 26.0, 25.2, 22.7, 14.1. MALDI-TOF-MS (*ferulic acid* as matrix): *m/z* calculated for $C_{336}H_{573}N_{21}O_{51}S_{12}$ $[M + Na]^+$ 6125.94, MW 6131.08; found 6129.89.

Generation-three phenolic wedge **10**. The general procedure of the Curtius reaction (*method 2*) was employed using 5-hydroxy-1,3-benzenediacrbonyl diazide **4** (104.9 mg, 0.452 mmol, 1.0 eq), **(G2W)$_{ene}$** (875.4 mg, 0.633 mmol, 1.4 eq), and anhydrous DMF (5 mL) to obtain a highly viscous, transparent oil as product **10** (827.7 mg, 0.270 mmol, 62% yield) after purification (40% EtOAc/hexane as mobile phase). TLC (40% EtOAc in hexane): R_f 0.38. ^{1}H NMR (500 MHz, CD_3COCD_3): δ 8.56 (s, 14H, NH), 8.25 (s, 1H), 7.30 (s, 6H), 7.22 (s, 1H), 7.00 (s, 12H), 6.92 (s, 1H), 5.89–5.83 (m, 8H), 5.02 (dd, *J* = 17.1, 10.2 Hz, 16H), 4.12 (q, *J* = 6.7 Hz, 28H), 3.94 (t, *J* = 6.3 Hz, 12H), 2.16 (q, *J* = 7.2 Hz, 16H), 1.80–1.72 (m, 30H), 1.70–1.60 (m, 12H), 1.50–1.27 (m, 98H). ^{13}C NMR (126 MHz, $CDCOCD_3$): δ 160.1, 158.2, 158.1, 153.6, 153.5, 140.65, 140.62, 137.9, 114.6, 100.7, 100.0, 99.9, 99.2, 67.6, 64.4, 64.3, 63.7, 29.8, 28.1, 25.9, 25.7. MALDI-TOF-MS (*dithranol* as matrix): *m/z* calculated for $C_{162}H_{240}N_{14}O_{35}Na$ $[M + Na]^+$ 2964.73, MW 2966.75; found 2966.58.

Generation-three dendron, **(G3W)$_{ene}$**. The procedure reported for **(G2W)$_{ene}$** was employed using 11-bromoundecanol (68.4 mg, 0.2721 mmol, 1.5 eq), K_2CO_3 (125.4 mg, 0.907 mmol, 5.0 eq), KI (9.0 mg, 0.0544 mmol, 0.3 eq), G3 phenolic wedge **10** (534.0 mg, 0.1814 mmol, 1.0 eq), and anhydrous acetone (8 mL) to obtain a gel-like, transparent prod-

uct (297.0 mg, 0.0954 mmol, 75% yield) after purification (40% EtOAc/Hexane as mobile. Phase). TLC (40% EtOAc in hexane): R_f 0.33. ^{1}H NMR (500 MHz, CD_3COCD_3): δ 8.60 (d, *J* = 12.2 Hz, 14H, NH), 7.30 (s, 7), 6.99 (s, 14H), 5.91–5.82 (m, 8H), 5.02 (dd, *J* = 17.1, 10.1 Hz, 16H), 4.12 (t, *J* = 6.8, 28H, overlapped triplets), 3.94 (t, *J* = 6.4 Hz, 14H), 3.55 (q, *J* = 5.7 Hz, 2H), 3.40 (t, 1H, OH), 2.16 (q, *J* = 7.2 Hz, 16H), 1.78–1.72 (m, 32H), 1.69–1.62 (m, 14H), 1.50–1.27 (m, 122H). ^{13}C NMR (126 MHz, CD_3COCD_3): δ 160.1, 158.1, 153.6, 153.5, 140.6, 137.9, 114.5, 100.7, 100.0, 99.1, 67.6, 64.4, 64.3, 63.7, 59.6, 29.8, 29.5, 28.1, 25.9, 25.7. MALDI-TOF-MS (*ferulic acid* as matrix): *m*/*z* calculated for $C_{173}H_{262}N_{14}O_{36}Na$ $[M + Na]^+$ 3134.90, MW 3137.05; found 3136.66.

Surface functionalized generation-three dendron, **G3W**. The general procedure of the thiol-ene click reaction was employed using **(G3W)$_{ene}$** (274.8 mg, 0.088 mmol, 1.0 eq), 1-octanethiol (184 µL, 1.059 mmol, 12.0 eq and AIBN (10 mg, 0.058 mmol, 0.8 eq), and anhydrous DCM (1.5 mL) to obtain a gel-like, transparent product (244 mg, 0.057 mmol, 65%) after purification (30% EtOAc/hexane as mobile phase). TLC (30% EtOAc in hexane): R_f 0.58. ^{1}H NMR (500 MHz, CD_3COCD_3): δ 8.58 (d, *J* = 7.1 Hz, 14H, NH), 7.30 (s, 7H), 7.01 (s, 14H), 4.12 (qn, *J* = 6.4 Hz, 28H, overlapped triplet), 3.94 (t, *J* = 6.2 Hz, 14H), 3.55 (q, *J* = 6.1 Hz, 2H), 3.42 (t, 1H, OH), 2.53 (q, *J* = 7.3 Hz, 32H), 1.80–1.72 (m, 16H), 0.89 (t, *J* = 6.8 Hz, 24H). The large aliphatic multiplet portion was not integrated. ^{13}C NMR (126 MHz, CD_3COCD_3): δ 160.1, 153.6, 153.5, 140.6, 100.7, 99.1, 67.6, 64.4, 64.3, 61.7, 32.9, 31.7, 31.6, 31.5, 29.6, 25.9, 25.8, 25.7, 25.0, 22.5, 13.5. MALDI-TOF-MS (*ferulic acid* as matrix): *m*/*z* calculated for $C_{237}H_{406}N_{14}O_{36}S_8Na$ $[M + Na]^+$ 4303.80, MW 4307.39; found 4307.95.

Generation-three dendrimer, **G3D**. The general procedure of the attachment of the dendron to the core was employed using 1,2,3-triisocyanatobenzene **6** (1.8 mg, 0.00918 mmol, 1.0 eq), **G3W** (118.0 mg, 0.02754 mmol, 3.0 eq), $BF_3.OEt_2$ (3 drops), and anhydrous DCM (1 mL) to obtain a highly viscous, transparent oil as the product (77.9 mg, 0.0060 mmol, 65% yield). TLC (5% acetone in DCM): R_f 0.22. ^{1}H NMR (500 MHz, CD_3COCD_3): δ 7.27 (s, 1H), 7.05 (s, 7H), 6.80 (s, 29H, broad), 4.15 (d, *J* = 5.2 Hz, 30H, overlapped triplets), 3.92 (s, 14H, broad triplets), 2.52 (q, *J* = 7.7 Hz, 32H), 0.90 (t, *J* = 13.0 Hz, 24H) (large aliphatic hydrocarbon portion was not integrated). ^{13}C NMR (126 MHz, CD_3COCD_3): δ 160.3, 153.5 (broad), 139.54, 139.48, 100.9, 99.9, 69.3, 68.0, 65.4, 65.2, 32.2, 32.0, 31.8, 29.9, 29.7, 29.6, 29.5, 29.4, 29.3, 29.24, 29.21, 29.0, 28.9, 28.6, 26.0, 25.9, 25.2, 22.7, 14.1. MALDI-TOF-MS: unsatisfactory data was obtained even with different matrices such as dithranol, ferulic acid, sinapic acid, HABA, HCCA, and DHB.

Supplementary Materials: The following are available online at https://www.mdpi.com/article/10.3390/reactions3010002/s1, Figure S1. Expanded structure of thiol-ene functionalized G1D (top) and its ball and stick (3D, hydrogen atoms are removed) model with lowest energy (bottom, 457.9 kJ/mol at 298 K). Red = oxygen atom, blue = nitrogen atom, yellow = sulfur atom. Figure S2. Expanded structure of thiol-ene functionalized G2D. Figure S3. Optimized geometry (with the hydrogen atoms removed) of thiol-ene functionalized G2D showing 3D ball and stick model (E = 750.0 kJ/mol at 298 K). Red = oxygen atom, blue = nitrogen atom, yellow = sulfur atom. Figure S4. Expanded structure of thiol-ene functionalized G3D. Figure S5. Optimized geometry (with the hydrogen atoms removed) of thiol-ene functionalized G3D showing 3D ball and stick model (E = 1735.4 kJ/mol at 298 K). Red = oxygen atom, blue = nitrogen atom, yellow = sulfur atom. Figure S6. 1H NMR spectrum (500 MHz, CD3COCD3, 298 K) of 5-hydroxy-1,3-benzenedicarbonyl diazide 4. Figure S7. 13C NMR spectrum (126 MHz, CD3COCD3, 298 K) of 5-hydroxy-1,3-benzenedicarbonyl diazide 4. Figure S8. 1H NMR spectrum (500 MHz, CD3COCD3, 298 K) of G2 phenolic wedge 9. Figure S9. 13C NMR spectrum (126 MHz, CD3COCD3, 298 K) of G2 phenolic wedge 9. Figure S10. 1H-1H COSY spectrum (500 MHz, CD3COCD3, 298 K) of G2 phenolic wedge 9. Figure S11. HSQC (1H-13C) spectrum (500 MHz, CD3COCD3, 298 K) of G2 phenolic wedge 9. Figure S12. 1H NMR spectrum (500 MHz, CD3COCD3, 298 K) of (G2W)ene. Figure S13. 13C NMR spectrum (126 MHz, CD3COCD3, 298 K) of (G2W)ene. Figure S14. COSY (1H-1H) spectrum (500 MHz, CD3COCD3, 298 K) of (G2W)ene. Figure S15. HSQC (1H-13C) spectrum (500 MHz, CD3COCD3, 298 K) of (G2W)ene. Figure S16. 1H NMR spectrum (500 MHz, CD3COCD3, 298 K) of G2W. Figure S17. 13C NMR spectrum (126 MHz, CD3COCD3, 298 K) of G2W. Figure S18. 1H NMR spectrum (500 MHz, CD3COCD3, 298 K) of G2D. Figure S19.

1H NMR spectrum (500 MHz, CDCl3, 298 K) of G2D. Figure S20. 13C NMR spectrum (126 MHz, CDCl3, 298 K) of G2D. Figure S21. 1H NMR spectrum (500 MHz, CD3COCD3, 298 K) of G3 phenolic wedge 10. Figure S22. 13C NMR spectrum (126 MHz, CD3COCD3, 298 K) of G3 phenolic wedge 10. Figure S23. 1H NMR spectrum (500 MHz, CD3COCD3, 298 K) of (G3W)ene. Figure S24. 13C NMR spectrum (126 MHz, CD3COCD3, 298 K) of (G3W)ene. Figure S25. 1H NMR spectrum (500 MHz, CD3COCD3, 298 K) of G3W. Figure S26. 13C NMR spectrum (126 MHz, CD3COCD3, 298 K) of G3W. Figure S27. 1H NMR spectrum (500 MHz, CDCl3, 298 K) of G3D. The aromatic region is expanded (at the top). Figure S28. 13C NMR spectrum (126 MHz, CDCl3, 298 K) of G3D. Figure S29. HSQC (1H-13C) spectrum (500 MHz, CDCl3, 298 K) of G3D showing (a) the aromatic and (b) the aliphatic region. Figure S30. COSY (1H-1H) spectrum (500 MHz, CDCl3, 298 K) of G3D. Figure S31. 2-D DOSY spectrum (CD3COCD3, 298 K, 500 MHz) of the surface functionalized generation-one dendrimer G1D, the diffusion coefficient D = 4.47 $\times$ 10^{-10} m^2/s. Figure S32. Showing fitting function after fitting with SimFit (T1/T2) analysis. The fitting curve for the peak at 8.612 ppm of G1D (CD3COCD3, 298 K, 500 MHz) is shown. Figure S33. 2-D DOSY spectrum (CDCl3, 298 K, 500 MHz) of the surface functionalized generation-two dendrimer G2D, the diffusion coefficient D = 1.857 $\times$ 10^{-10} m^2/s. Figure S34. Showing fitting function after fitting with SimFit (T1/T2) analysis. The fitting curve for the peak at 7.312 ppm of G2D (CDCl3, 298 K, 500 MHz) is shown. Figure S35. 2-D DOSY spectrum (CDCl3, 298 K, 500 MHz) of the surface functionalized generation-two dendrimer G3D, the diffusion coefficient D = 1.381 $\times$ 10^{-10} m^2/s. Figure S36. Showing fitting function after fitting with SimFit (T1/T2) analysis. The fitting curve for the peak at 7.047 ppm of G3D (CDCl3, 298 K, 500 MHz) is shown. Figure S37. HRMS (ESI-LTQ-Orbitrap) of linking agent 4. Figure S38. LRMS (MALDI-TOF-MS) of generation – two phenolic wedge 9. Figure S39. LRMS (MALDI-TOF-MS) of generation – two dendron with alkene periphery, (G2W)ene. Figure S40. LRMS (MALDI-TOF-MS) of generation – two dendron with alkene periphery, G2W. Figure S41. LRMS (MALDI-TOF-MS) of generation – two dendron with alkene periphery, G2D. Figure S42. LRMS (MALDI-TOF-MS) of generation – three phenolic wedge 10. Figure S43. LRMS (MALDI-TOF-MS) of generation – three dendron with alkene periphery, (G3W)ene. Figure S45. LRMS (MALDI-TOF-MS) of generation-two dendron with alkene periphery, G3W. Figure S46. FT-IR spectrum of 5-hydroxy-1,3-benzenedicarbonyl diazide 4. Figure S47. Figure S47. (a) FT-IR spectrum of 1,3,5-triisocyanatobenzene 6.(b) FT-IR spectrum of G2 phenolic wedge 9. Figure S48. FT-IR spectrum of (G2W)ene. Figure S49. FT-IR spectrum of G2W. Figure S50. FT-IR spectrum of G2D. Figure S51. FT-IR spectrum of (G3W)ene. Figure S52. FT-IR spectrum of G3W. Figure S53. FT-IR spectrum of G3D. Figure S54. UV-Vis spectrum of G3D (measured at 1.3 mM concentration). Figure S55. Emission spectrum of G3D (measured at 1.3 mM concentration). The data of the excitation portion (317 nm – 331 nm) are removed for clarity.

Author Contributions: Conceptualization, R.T.T.; methodology, D.P.P.; investigation, D.P.P.; writing—original draft preparation, D.P.P.; writing—review and editing, R.T.T. and D.P.P.; supervision, R.T.T. All authors have read and agreed to the published version of the manuscript.

Funding: This research received no external funding.

Institutional Review Board Statement: Not applicable.

Informed Consent Statement: Not applicable.

Data Availability Statement: The data presented in this study are available upon request from the corresponding author. The data are not publicly available because of the lack of dedicated server.

Acknowledgments: We acknowledge the Department of Chemistry and Biochemistry of Miami University.

Conflicts of Interest: The authors declare no conflict of interest.

References

1. Sowinska, M.; Urbanczyk-Lipkowska, Z. Advances in the Chemistry of Dendrimers. *New J. Chem.* **2014**, *38*, 2168–2203. [CrossRef]
2. Fréchet, J.M.J. Functional Polymers and Dendrimers: Reactivity, Molecular Architecture, and Interfacial Energy. *Science* **1994**, *263*, 1710–1715. [CrossRef]
3. Sandra García-Gallego, M.M. *Dendrimer Chemistry: Synthetic Approaches Towards Complex Architectures*; Croydon Royal Society of Chemistry: London, UK, 2020.
4. Tomalia, D.A.; Fréchet, J.M.J. Discovery of Dendrimers and Dendritic Polymers: A Brief Historical Perspective. *J. Polym. Sci. Part A Polym. Chem.* **2002**, *40*, 2719–2728. [CrossRef]

5. Sebestik, J.; Reinis, M.; Jezek, J. *Biomedical Applications of Peptide-, Glyco-, and Glycopeptide Dendrimers, and Analogous Dendrimeric Structurrs*; Springer: Berlin/Heidelberg, Germany, 2012.
6. Astruc, D.; Boisselier, E.; Ornelas, C. Dendrimers Designed for Functions: From Physical, Photophysical, and Supramolecular Properties to Applications in Sensing, Catalysis, Molecular Electronics, Photonics, and Nanomedicine. *Chem. Rev.* **2010**, *110*, 1857–1959. [CrossRef]
7. Sharma, A.; Liaw, K.; Sharma, R.; Spriggs, T.; Appiani La Rosa, S.; Kannan, S.; Kannan, R.M. Dendrimer-Mediated Targeted Delivery of Rapamycin to Tumor-Associated Macrophages Improves Systemic Treatment of Glioblastoma. *Biomacromolecules* **2020**, *21*, 5148–5161. [CrossRef]
8. Takeda, S.; Nishimura, T.; Umezaki, K.; Kubo, A.; Yanase, M.; Sawada, S.I.; Sasaki, Y.; Akiyoshi, K. Synthesis and Function of Amphiphilic Glucan Dendrimers as Nanocarriers for Protein Delivery. *Biomater. Sci.* **2019**, *7*, 1617–1622. [CrossRef]
9. Wang, X.Q.; Wang, W.; Li, W.J.; Chen, L.J.; Yao, R.; Yin, G.Q.; Wang, Y.X.; Zhang, Y.; Huang, J.; Tan, H.; et al. Dual Stimuli-Responsive Rotaxane-Branched Dendrimers with Reversible Dimension Modulation. *Nat. Commun.* **2018**, *9*, 3190. [CrossRef]
10. Wang, Y.; Zhu, X. Nanofabrication within Unimolecular Nanoreactors. *Nanoscale* **2020**, *12*, 12698–12711. [CrossRef]
11. Watabe, T.; Ishizuki, K.; Aoki, D.; Otsuka, H. Mechanochromic Dendrimers: The Relationship between Primary Structure and Mechanochromic Properties in the Bulk. *Chem. Commun.* **2019**, *55*, 6831–6834. [CrossRef]
12. Xu, X.; Zhang, P.; Wu, B.; Xing, Y.; Shi, K.; Fang, W.; Yu, H.; Wang, G. Photochromic Dendrimers for Photoswitched Solid-To-Liquid Transitions and Solar Thermal Fuels. *ACS Appl. Mater. Interfaces* **2020**, *12*, 50135–50142. [CrossRef]
13. Astruc, D.; Chardac, F. Dendritic Catalysts and Dendrimers in Catalysis. *Chem. Rev.* **2001**, *101*, 2991–3023. [CrossRef]
14. Ghobril, C.; Rodriguez, E.K.; Nazarian, A.; Grinstaff, M.W. Recent Advances in Dendritic Macromonomers for Hydrogel Formation and Their Medical Applications. *Biomacromolecules* **2016**, *17*, 1235–1252. [CrossRef]
15. Loch, A.S.; Stoltzfus, D.M.; Burn, P.L.; Shaw, P.E. High-Sensitivity Poly(Dendrimer)-Based Sensors for the Detection of Explosives and Taggant Vapors. *Macromolecules* **2020**, *53*, 1652–1664. [CrossRef]
16. Lyu, Z.; Ding, L.; Tintaru, A.; Peng, L. Self-Assembling Supramolecular Dendrimers for Biomedical Applications: Lessons Learned from Poly(Amidoamine) Dendrimers. *Acc. Chem. Res.* **2020**, *53*, 2936–2949. [CrossRef]
17. Majoral, J.P.; Mignani, S.M.; Shi, X.; Rodrigues, J.M.; Muñoz-Fernández, M.Á.; Ceña, V.; Roy, R. Dendrimers towards Translational Nanotherapeutics: Concise Key Step Analysis. *Bioconjug. Chem.* **2020**, *31*, 2060–2071.
18. Jiang, W.; Stolterfoht, M.; Jin, H.; Paul, L.B. Hole-Transporting Poly(dendrimer)s as Electron Donors for Low Donor Organic Solar Cells with Efficient Charge Transport. *Macromolecules* **2020**, *53*, 2902–2911. [CrossRef]
19. Mignani, S.; Shi, X.; Steinmetz, A.; Majoral, J.P. Multivalent Copper(II)-Conjugated Phosphorus Dendrimers with Noteworthy in Vitro and in Vivo Antitumor Activities: A Concise Overview. *Mol. Pharm.* **2021**, *18*, 65–73. [CrossRef]
20. Puttock, E.V.; Ranasinghe, C.S.K.; Babazadeh, M.; Jang, J.; Huang, D.M.; Tsuchiya, Y.; Adachi, C.; Burn, P.L.; Shaw, P.E. Solution-Processed Dendrimer-Based TADF Materials for Deep-Red OLEDs. *Macromolecules* **2020**, *53*, 10375–10385. [CrossRef]
21. Tomalia, D.A.; Baker, H.; Hall, M.; Kallos, G.; Martin, S.; Ryder, J.; Smith, P. Dendritic Macromolecules:1 Synthesis of Starburst Dendrimers. *Macromolecules* **1986**, *19*, 2466–2468. [CrossRef]
22. Agrahari, A.K.; Singh, A.S.; Mukherjee, R.; Tiwari, V.K. An Expeditious Click Approach towards the Synthesis of Galactose Coated Novel Glyco-Dendrimers and Dentromers Utilizing a Double Stage Convergent Method. *RSC Adv.* **2020**, *10*, 31553–31562. [CrossRef]
23. Thomas, B.; Pifferi, C.; Daskhan, G.C.; Fiore, M.; Berthet, N.; Renaudet, O. Divergent and Convergent Synthesis of GalNAc-Conjugated Dendrimers Using Dual Orthogonal Ligations. *Org. Biomol. Chem.* **2015**, *13*, 11529–11538. [CrossRef]
24. Zhang, Y.; Üçüncü, M.; Gambardella, A.; Baibek, A.; Geng, J.; Zhang, S.; Clavadetscher, J.; Litzen, I.; Bradley, M.; Lilienkampf, A. Bioorthogonal Swarming: In Situ Generation of Dendrimers. *J. Am. Chem. Soc.* **2020**, *142*, 21615–21621. [CrossRef]
25. Zhou, H.Y.; Zong, Q.S.; Han, Y.; Chen, C.F. Recent Advances in Higher Order Rotaxane Architectures. *Chem. Commun.* **2020**, *56*, 9916–9936. [CrossRef]
26. El Hankari, S.; Katir, N.; Collière, V.; Coppel, Y.; Bousmina, M.; Majoral, J.P.; El Kadib, A. Urea-Assisted Cooperative Assembly of Phosphorus Dendrimer-Zinc Oxide Hybrid Nanostructures. *New J. Chem.* **2019**, *43*, 2141–2147. [CrossRef]
27. Farabi, K.; Manabe, Y.; Ichikawa, H.; Miyake, S.; Tsutsui, M.; Kabayama, K.; Yamaji, T.; Tanaka, K.; Hung, S.C.; Fukase, K. Concise and Reliable Syntheses of Glycodendrimers via Self-Activating Click Chemistry: A Robust Strategy for Mimicking Multivalent Glycan-Pathogen Interactions. *J. Org. Chem.* **2020**, *85*, 16014–16023. [CrossRef]
28. Kaufman, E.A.; Tarallo, R.; Elacqua, E.; Carberry, T.P.; Weck, M. Synthesis of Well-Defined Bifunctional Newkome-Type Dendrimers. *Macromolecules* **2017**, *50*, 4897–4905. [CrossRef]
29. Li, W.J.; Hu, Z.; Xu, L.; Wang, X.Q.; Wang, W.; Yin, G.Q.; Zhang, D.Y.; Sun, Z.; Li, X.; Sun, H.; et al. Rotaxane-Branched Dendrimers with Enhanced Photosensitization. *J. Am. Chem. Soc.* **2020**, *142*, 16748–16756. [CrossRef]
30. Milenin, S.A.; Cherkaev, G.V.; Demchenko, N.V.; Serkova, E.S.; Krasnova, I.Y.; Selezneva, E.V.; Buzin, M.I.; Bakirov, A.V.; Vasil'ev, V.G.; Shifrina, Z.B.; et al. Influence of the Growing Flexible Shell on the Molecular Behavior of Hybrid Dendrimers. *Macromolecules* **2020**, *53*, 9706–9716. [CrossRef]
31. Molina, N.; Nájera, F.; Guadix, J.A.; Perez-Pomares, J.M.; Vida, Y.; Perez-Inestrosa, E. Synthesis of Amino Terminal Clicked Dendrimers. Approaches to the Application as a Biomarker. *J. Org. Chem.* **2019**, *84*, 10197–10208. [CrossRef]
32. Sharma, R.; Kottari, N.; Chabre, Y.M.; Abbassi, L.; Shiao, T.C.; Roy, R. A Highly Versatile Convergent/Divergent "Onion Peel" Synthetic Strategy toward Potent Multivalent Glycodendrimers. *Chem. Commun.* **2014**, *50*, 13300–13303. [CrossRef]

33. Stadler, A.M. Structural Features of Fréchet-Type Dendrons and Dendrimers in Single Crystals. *Cryst. Growth Des.* **2010**, *10*, 5050–5065. [CrossRef]
34. Bruchmann, B. Dendritic Polymers Based on Urethane Chemistry—Syntheses and Applications. *Macromol. Mater. Eng.* **2007**, *292*, 981–992. [CrossRef]
35. Etcalf, R.O.L.M. General Info of Isocyanates and Their Handling. *Ullmann's Encycl. Ind. Chem.* **2012**, 264–322. [CrossRef]
36. Spindler, R.; Fréchet, J.M.J. Synthesis and Characterization of Hyperbranched Polyurethanes Prepared from Blocked Isocyanate Monomers by Step-Growth Polymerization. *Macromolecules* **1993**, *26*, 4809–4813. [CrossRef]
37. Spindler, R.; Fréchet, J.M.J. Two-Step Approach towards the Accelerated Synthesis of Dendritic Macromolecules. *J. Chem. Soc. Perkin Trans. 1* **1993**, 913–918. [CrossRef]
38. Kumar, A.; Ramakrishnan, S. A Novel One-Pot Synthesis of Hyperbranched Polyurethanes. *J. Chem. Soc. Chem. Comm.* **1993**, 1453–1454. [CrossRef]
39. Newkome, G.R.; Yao, Z.Q.; Baker, G.R.; Gupta, V.K. Cascade Molecules: A New Approach to Micelles. *J. Org. Chem.* **1985**, *50*, 2003–2004. [CrossRef]
40. Duan, X.; Griffith, C.M.; Dube, M.A.; Sheardown, H. Novel Dendrimer Based Polyurethanes for PEO incorporation. *Journal of Biomaterials Sc.* **2012**, *13*, 667–689. [CrossRef]
41. Clark, A.M.; Echenique, J.; Haddelton, D.M.; Straw, T.A.; Taylor, P.C. A Nonisocyanate Route to Monodisperse Branched Polyurethanes. *J. Org. Chem.* **2001**, *66*, 8687–8689. [CrossRef] [PubMed]
42. Goodwin, A.P.; Lam, S.S.; Fréchet, J.M.J. Rapid, Efficient Synthesis of Heterofunctional Biodegradable Dendrimers. *J. Am. Chem. Soc.* **2007**, *129*, 6994–6995. [CrossRef]
43. Rannard, S.P.; Davis, N.J.; Herbert, I. Synthesis of Water Soluble Hyperbranched Polyurethanes Using Selective Activation of AB2 Monomers. *Macromolecules* **2004**, *37*, 9418–9430. [CrossRef]
44. Peerlings, H.W.I.; Van Benthem, R.A.T.M.; Meijer, E.W. Fast and Convenient Construction of Carbamate/Urea-Based Dendrimers with a Diisocyanate Building Block. *J. Polym. Sci. Part A Polym. Chem.* **2001**, *39*, 3112–3120. [CrossRef]
45. Tong, Q.S.; Xu, W.; Huang, Q.Y.; Zhang, Y.R.; Shi, X.X.; Huang, H.; Li, H.J.; Du, J.Z.; Wang, J. Multi-Stimuli Responsive Poly(amidoamine) Dendrimers with Peripheral: N -Dialkylaminoethyl Carbamate Moieties. *Polym. Chem.* **2019**, *10*, 656–662. [CrossRef]
46. Abdelrehim, M.; Komber, H.; Langenwalter, J.; Voit, B.; Bruchmann, B. Synthesis and Characterization of Hyperbranched Poly(urea-urethanes) Based on AA* and B2B* Monomers. *J. Polym. Sci. Part A Polym. Chem.* **2004**, *42*, 3062–3081. [CrossRef]
47. Gomez, I.J.; Arnaiz, B.; Cacioppo, M.; Arcudi, F.; Prato, M. Nitrogen-Doped Carbon Nanodots for Bioimaging and Delivery of Paclitaxel. *J. Mater. Chem. B* **2018**, *6*, 5540–5548. [CrossRef]
48. Mohamad Ali, B.; Velavan, B.; Sudhandiran, G.; Sridevi, J.; Sultan Nasar, A. Radical Dendrimers: Synthesis, Anti-Tumor Activity and Enhanced Cytoprotective Performance of TEMPO Free Radical Functionalized Polyurethane Dendrimers. *Eur. Polym. J.* **2020**, *122*, 109354. [CrossRef]
49. Ashok Kumar, K.; Sultan Nasar, A.; Mohamad Ali, B.; Bargathulla, I.; Sathiyaraj, S. Elimination of 50% Iodine and Excellent Performance of Dye-Sensitized Solar Cell Enabled by Tempo Radical Dendrimer−iodide Dual Redox Systems. *ACS Appl. Energy Mater.* **2020**, *3*, 10506–10514.
50. Sathiyaraj, S.; Kumar, K.A.; Jailani Shanavas, A.K.; Sultan Nasar, A.S. The First Example of Bisindole-Based Polyurethane Dendrimers: Synthesis and Performance in DSSC. *ChemistrySelect* **2017**, *2*, 7108–7116. [CrossRef]
51. Matsumura, S.; Hlil, A.R.; Lepiller, C.; Gaudet, J.; Guay, D.; Shi, Z.; Holdcroft, S.; Hay, A.S. Stability and Utility of Pyridyl Disulfide Functionality in RAFT and Conventional Radical Polymerizations. *J. Polym. Sci. Part A Polym. Chem.* **2008**, *46*, 7207–7224.
52. Veerapandian, S.; Amudha, S.; Suthanthiraraj, S.A.; Rahman, M.A.; Nasar, A.S. Enhanced Performance of a Nanocrystalline Dye-Sensitized Solar Cell Based on Polyurethane Dendrimers. *RSC Adv.* **2015**, *5*, 31404–31409. [CrossRef]
53. Grayson, S.M.; Fréchet, J.M.J. Convergent Dendrons and Dendrimers. *Chem. Rev.* **2001**, *101*, 3819–3867. [CrossRef]
54. Hawker, C.J.; Fréchet, J.M.J. Preparation of Polymers with Controlled Molecular Architecture. A New Convergent Approach to Dendritic Macromolecules. *J. Am. Chem. Soc.* **1990**, *112*, 7638–7647. [CrossRef]
55. Kowalczyk, W.; Mascaraque, A.; Sánchez-Navarro, M.; Rojo, J.; Andreu, D. Convergent Synthesis of Glycodendropeptides by Click Chemistry Approaches. *Eur. J. Org. Chem.* **2012**, *24*, 4565–4573. [CrossRef]
56. López-Méndez, L.J.; Cuéllar-Ramírez, E.E.; Cabrera-Quiñones, N.C.; Rojas-Aguirre, Y.; Guadarrama, P. Convergent Click Synthesis of Macromolecular Dendritic β-Cyclodextrin Derivatives as Non-Conventional Drug Carriers: Albendazole as Guest Model. *Int. J. Biol. Macromol.* **2020**, *164*, 1704–1714. [CrossRef] [PubMed]
57. Moreno, P.; Quéléver, G.; Peng, L. Synthesis of Poly(aminoester) Dendrimers via "click" Chemistry in Combination with the Divergent and Convergent Strategies. *Tetrahedron Lett.* **2015**, *56*, 4043–4046. [CrossRef]
58. Golshan, M.; Rostami-Tapeh-Esmail, E.; Salami-Kalajahi, M.; Roghani-Mamaqani, H. A Review on Synthesis, Photophysical Properties, and Applications of Dendrimers with Perylene Core. *Eur. Polym. J.* **2020**, *137*, 109933. [CrossRef]
59. Wang, L.; Kiemle, D.J.; Boyle, C.J.; Connors, E.L.; Gitsov, I. "Click" Synthesis of Intrinsically Hydrophilic Dendrons and Dendrimers Containing Metal Binding Moieties at Each Branching Unit. *Macromolecules* **2014**, *47*, 2199–2213. [CrossRef]
60. Sehad, C.; Shiao, T.C.; Sallam, L.M.; Azzouz, A.; Roy, R. Effect of Dendrimer Generation and Aglyconic Linkers on the Binding Properties of Mannosylated Dendrimers Prepared by a Combined Convergent and Onion Peel Approach. *Molecules* **2018**, *23*, 1890. [CrossRef]

61. Meyhoff, U.; Riber, U.; Boas, U. Convergent Synthesis of Degradable Dendrons Based on L-Malic Acid. *New J. Chem.* **2015**, *39*, 1161–1171. [CrossRef]
62. Guizzardi, R.; Vacchini, M.; Santambrogio, C.; Cipolla, L. Convergent Dendrimer Synthesis by Olefin Metathesis and Studies toward Glycoconjugation. *Can. J. Chem.* **2017**, *95*, 1008–1012. [CrossRef]
63. Bondareva, J.; Kolotylo, M.; Rozhkov, V.; Burilov, V.; Lukin, O. A Convergent Approach to Sulfonimide-Based Dendrimers and Dendrons. *Tetrahedron Lett.* **2020**, *61*, 152011. [CrossRef]
64. Ray, A.; Khan, S. Convergent Synthesis of Novel Mono- and Di-Substituted 1,2-Isopropylideneglucofuranose Appended Dendrimers with a Ferrocene Core and Their Electrochemical Studies. *Synlett* **2018**, *29*, 1367–1372. [CrossRef]
65. Miller, T.M.; Neenan, T.X. Convergent Synthesis of Monodisperse Dendrimers Based upon 1,3,5-Trisubstituted Benzenes. *Chem. Mater.* **1990**, *2*, 346–349. [CrossRef]
66. Hsieh, C.W.; Chen, Y.H.; Jeng, R.J.; Dai, S.H.A. Convergent Synthesis of Polyimide Dendrimers from an ABB′ Intermediate. *Adv. Mater. Res.* **2013**, *716*, 438–442. [CrossRef]
67. Enciso, A.E.; Abid, Z.M.; Simanek, E.E. Rapid, Semi-Automated Convergent Synthesis of Low Generation Triazine Dendrimers Using Microwave Assisted Reactions. *Polym. Chem.* **2014**, *5*, 4635–4640. [CrossRef]
68. Han, S.C.; Kim, J.H.; Lee, J.W. Convergent Synthesis of PAMAM Dendrimers Containing Tetra(ethyleneoxide) at Core Using Click Chemistry. *Bull. Korean Chem. Soc.* **2012**, *33*, 3501–3504. [CrossRef]
69. Akiyama, H.; Miyashita, K.; Hari, Y.; Obika, S.; Imanishi, T. Synthesis of Novel Polyesteramine Dendrimers by Divergent and Convergent Methods. *Tetrahedron* **2013**, *69*, 6810–6820. [CrossRef]
70. Joosten, A.; Schneider, J.P.; Lepage, M.L.; Tarnus, C.; Bodlenner, A.; Compain, P. A Convergent Strategy for the Synthesis of Second-Generation Iminosugar Clusters Using "Clickable" Trivalent Dendrons. *Eur. J. Org. Chem.* **2014**, *2014*, 1866–1872. [CrossRef]
71. Laurent, B.A.; Grayson, S.M. Synthesis of Cyclic Dendronized Polymers via Divergent "Graft- from" and Convergent Click "Graft-to" Routes: Preparation of Modular Toroidal Macromolecules. *J. Am. Chem. Soc.* **2011**, *133*, 13421–13429. [CrossRef]
72. Jee, J.A.; Spagnuolo, L.A.; Rudick, J.G. Convergent Synthesis of Dendrimers via the Passerini Three-Component Reaction. *Org. Lett.* **2012**, *14*, 3292–3295. [CrossRef]
73. Feast, W.J.; Rannard, S.P.; Stoddart, A. Selective Convergent Synthesis of Aliphatic Polyurethane Dendrimers. *Macromolecules* **2003**, *36*, 9704–9706. [CrossRef]
74. Stoddart, A.; Feast, W.J.; Rannard, S.P. Synthesis and Thermal Studies of Aliphatic Polyurethane Dendrimers: A Geometric Approach to the Flory-Fox Equation for Dendrimer Glass Transition Temperature. *Soft Matter* **2012**, *8*, 1096–1108. [CrossRef]
75. Reemers, S.; Mourran, A.; Keul, H.; Möller, M. Novel Route to Dendritic Structures and Their Application for Surface Modification. *J. Polym. Sci. Part A Polym. Chem.* **2006**, *44*, 1372–1386. [CrossRef]
76. Hoyle, C.E.; Bowman, C.N. Thiol-Ene Click Chemistry. *Angew. Chem.-Int. Ed.* **2010**, *49*, 1540–1573. [CrossRef] [PubMed]
77. Dondoni, A. The Emergence of Thiol-Ene Coupling as a Click Process for Materials and Bioorganic Chemistry. *Angew. Chem.-Int. Ed.* **2008**, *47*, 8995–8997. [CrossRef] [PubMed]
78. Sharma, A.; Sharma, R.; Zhang, Z.; Liaw, K.; Kambhampati, S.P.; Porterfield, J.E.; Lin, K.C.; DeRidder, L.B.; Kannan, S.; Kannan, R.M. Dense Hydroxyl Polyethylene Glycol Dendrimer Targets Activated Glia in Multiple CNS Disorders. *Sci. Adv.* **2020**, *6*, 1–15. [CrossRef]
79. Montañez, M.I.; Campos, L.M.; Antoni, P.; Hed, Y.; Walter, M.V.; Krull, B.T.; Khan, A.; Hult, A.; Hawker, C.J.; Malkoch, M. Accelerated Growth of Dendrimers via Thiol-Ene and Esterification Reactions. *Macromolecules* **2010**, *43*, 6004–6013. [CrossRef]
80. Fuentes-Paniagua, E.; Hernández-Ros, J.M.; Sánchez-Milla, M.; Camero, M.A.; Maly, M.; Pérez-Serrano, J.; Copa-Patiño, J.L.; Sánchez-Nieves, J.; Soliveri, J.; Gómez, R.; et al. Carbosilane Cationic Dendrimers Synthesized by Thiol-Ene Click Chemistry and Their Use as Antibacterial Agents. *RSC Adv.* **2014**, *4*, 1256–1265. [CrossRef]
81. Bi, X.; Liang, A.; Tan, Y.; Maturavongsadit, P.; Higginbothem, A.; Gado, T.; Gramling, A.; Bahn, H.; Wang, Q. Thiol-Ene Crosslinking Polyamidoamine Dendrimer-Hyaluronic Acid Hydrogel System for Biomedical Applications. *J. Biomater. Sci. Polym. Ed.* **2016**, *27*, 743–757. [CrossRef]
82. Sharma, R.; Zhang, I.; Shiao, T.C.; Pavan, G.M.; Maysinger, D.; Roy, R. Low Generation Polyamine Dendrimers Bearing Flexible Tetraethylene Glycol as Nanocarriers for Plasmids and SiRNA. *Nanoscale* **2016**, *8*, 5106–5119. [CrossRef]
83. Kaya, N.U.; Du Prez, F.E.; Badi, N. Multifunctional Dendrimer Formation Using Thiolactone Chemistry. *Macromol. Chem. Phys.* **2017**, *218*, 1600575. [CrossRef]
84. Bagul, R.S.; Hosseini, M.M.; Shiao, T.C.; Roy, R. "Onion Peel" Glycodendrimer Syntheses Using Mixed Triazine and Cyclotriphosphazene Scaffolds. *Can. J. Chem.* **2017**, *95*, 975–983. [CrossRef]
85. Granskog, V.; Andrén, O.C.J.; Cai, Y.; González-Granillo, M.; Felländer-Tsai, L.; Von Holst, H.; Haldosen, L.A.; Malkoch, M. Linear Dendritic Block Copolymers as Promising Biomaterials for the Manufacturing of Soft Tissue Adhesive Patches Using Visible Light Initiated Thiol-Ene Coupling Chemistry. *Adv. Funct. Mater.* **2015**, *25*, 6596–6605. [CrossRef]
86. Han, Y.; Zhou, X.; Qian, Y.; Hu, H.; Zhou, Z.; Liu, X.; Tang, J.; Shen, Y. Hypoxia-Targeting Dendritic MRI Contrast Agent Based on Internally Hydroxy Dendrimer for Tumor Imaging. *Biomaterials* **2019**, *213*, 119195. [CrossRef] [PubMed]
87. Zhang, Y.; Andrén, O.C.J.; Nordström, R.; Fan, Y.; Malmsten, M.; Mongkhontreerat, S.; Malkoch, M. Off-Stoichiometric Thiol-Ene Chemistry to Dendritic Nanogel Therapeutics. *Adv. Funct. Mater.* **2019**, *29*, 1806693. [CrossRef]

88. Zhang, J.; Liu, C.; Cheng, J.; Miao, M.; Zhang, D. Simultaneous Toughening and Strengthening of Diglycidyl Ether of Bisphenol-a Using Epoxy-Ended Hyperbranched Polymers Obtained from Thiol-Ene Click Reaction. *Polym. Eng. Sci.* **2018**, *58*, 1703–1709. [CrossRef]
89. Hoff, E.A.; De Hoe, G.X.; Mulvaney, C.M.; Hillmayer, M.A.; Alabi, C.A. Thiol-Ene Networks from Sequence-Defined Polyurethane Macromers. *J. Am. Chem. Soc.* **2020**, *43*, 6004–6013. [CrossRef]
90. Soiberman, U.; Kambhampati, S.P.; Wu, T.; Mishra, M.K.; Oh, Y.; Sharma, R.; Wang, J.; Al Towerki, A.E.; Yiu, S.; Stark, W.J.; et al. Subconjunctival Injectable Dendrimer-Dexamethasone Gel for the Treatment of Corneal Inflammation. *Biomaterials* **2017**, *125*, 38–53. [CrossRef]
91. Aoki, K.; Imanishi, R.; Yamada, M. Novel Dendritic Polyenes for Application to Tailor-Made Thiol-Ene Photopolymers with Excellent UV-Curing Performance. *Prog. Org. Coat.* **2016**, *100*, 105–110. [CrossRef]
92. Quintana, S.; García, M.Á.; Marina, M.L.; Gómez, R.; de la Mata, F.J.; Ortega, P. Synthesis of Chiral Carbosilane Dendrimers with L-Cysteine and N-Acetyl-L-Cysteine on Their Surface and Their Application as Chiral Selectors for Enantiomer Separation by Capillary Electrophoresis. *Tetrahedron Asymmetry* **2017**, *28*, 1797–1802. [CrossRef]
93. Naguib, H.; Cao, X.; Gao, H. Synthesize Hyperbranched Polymers Carrying Two Reactive Handles via CuAAC Reaction and Thiol–Ene Chemistry. *Macromol. Chem. Phys.* **2019**, *220*, 1900221. [CrossRef]
94. Wang, J.; Cooper, R.C.; Yang, H. Polyamidoamine Dendrimer Grafted with an Acid-Responsive Charge-Reversal Layer for Improved Gene Delivery. *Biomacromolecules* **2020**, *21*, 4008–4016. [CrossRef] [PubMed]
95. Ortega, P.; Gómez, R.; De La Mata, F.J. Thiol Ended Carbosilane Dendrimers. A Multivalent Platform for the Binding of Molecules of Biological Interest. *Tetrahedron Lett.* **2015**, *56*, 5299–5302. [CrossRef]
96. Rissing, C.; Son, D.Y. Application of Thiol—Ene Chemistry to the Preparation of Carbosilane—Thioether Dendrimers. *Organometallics* **2009**, *28*, 3167–3172. [CrossRef]
97. Zhang, Z.; Feng, S.; Zhang, J. Facile and Efficient Synthesis of Carbosiloxane Dendrimers via Orthogonal Click Chemistry between Thiol and Ene. *Macromol. Rapid Commun.* **2016**, *37*, 318–322. [CrossRef]
98. Cakir, N.; Tunca, U.; Hizal, G.; Durmaz, H. Heterofunctionalized Multiarm Star Polymers via Sequential Thiol-Para-Fluoro and Thiol-Ene Double "Click" Reactions. *Macromol. Chem. Phys.* **2016**, *217*, 636–645. [CrossRef]
99. Kaga, S.; Gevrek, T.N.; Sanyal, A.; Sanyal, R. Synthesis and Functionalization of Dendron-Polymer Conjugate Based Hydrogels via Sequential Thiol-Ene "Click" Reactions. *J. Polym. Sci. Part A Polym. Chem.* **2016**, *54*, 926–934. [CrossRef]
100. Antoni, P.; Robb, M.J.; Campos, L.; Montanez, M.; Hult, A.; Malmström, E.; Malkoch, M.; Hawker, C.J. Pushing the Limits for Thiol-Ene and CuAAC Reactions: Synthesis of a 6th Generation Dendrimer in a Single Day. *Macromolecules* **2010**, *43*, 6625–6631. [CrossRef]
101. Lo Conte, M.; Robb, M.J.; Hed, Y.; Marra, A.; Malkoch, M.; Hawker, C.J.; Dondoni, A. Exhaustive Glycosylation, Pegylation, and Glutathionylation of a [G4]-Ene48 Dendrimer via Photoinduced Thiol-Ene Coupling. *J. Polym. Sci. Part A Polym. Chem.* **2011**, *49*, 4468–4475. [CrossRef]
102. Fuentes-Paniagua, E.; Peña-González, C.E.; Galán, M.; Gómez, R.; De La Mata, F.J.; Sánchez-Nieves, J. Thiol-Ene Synthesis of Cationic Carbosilane Dendrons: A New Family of Synthons. *Organometallics* **2013**, *32*, 1789–1796. [CrossRef]
103. Robb, M.J.; Hawker, C.J. "Click" Chemistry in Polymer Science: CuAAC and Thiol-Ene Coupling for the Synthesis and Functionalization of Macromolecules. *Mater. Sci. Technol.* **2012**, 923–972. [CrossRef]
104. Sharma, R.; Naresh, K.; Chabre, Y.M.; Rej, R.; Saadeh, N.K.; Roy, R. Onion Peel Dendrimers: A Straightforward Synthetic Approach towards Highly Diversified Architectures. *Polym. Chem.* **2014**, *5*, 4321–4331. [CrossRef]
105. Ghirardello, M.; Öberg, K.; Staderini, S.; Renaudet, O.; Berthet, N.; Dumy, P.; Hed, Y.; Marra, A.; Malkoch, M.; Dondoni, A. Thiol-Ene and Thiol-Yne-Based Synthesis of Glycodendrimers as Nanomolar Inhibitors of Wheat Germ Agglutinin. *J. Polym. Sci. Part A Polym. Chem.* **2014**, *52*, 2422–2433. [CrossRef]
106. Galán, M.; Sánchez Rodríguez, J.; Jiménez, J.L.; Relloso, M.; Maly, M.; De La Mata, F.J.; Muñoz-Fernández, M.A.; Gómez, R. Synthesis of New Anionic Carbosilane Dendrimers via Thiol-Ene Chemistry and Their Antiviral Behaviour. *Org. Biomol. Chem.* **2014**, *12*, 3222–3237. [CrossRef] [PubMed]
107. Kottari, N.; Chabre, Y.M.; Shiao, T.C.; Rej, R.; Roy, R. Efficient and Accelerated Growth of Multifunctional Dendrimers Using Orthogonal Thiol–Ene and SN2 Reactions. *Chem. Commun.* **2014**, *50*, 1983–1985. [CrossRef]
108. Jeong, H.J.; Kim, B.K. Shape Memory Hyperbranched Polyurethanes via Thiol-Ene Click Chemistry. *React. Funct. Polym.* **2017**, *116*, 92–100. [CrossRef]
109. Han, W. Application of Thiol-Ene "Click" Chemistry to Preparation of Hyperbranched Polyurethane Acrylate Oligomers Containing Carboxyl Groups. *J. Photopolym. Sci. Technol.* **2015**, *28*, 419–427. [CrossRef]
110. Puapaiboon, U.; Taylor, R.T. Characterization and Monitoring Reaction of Polyurethane Dendritic Wedges and Dendrimers Using Matrix-Assisted Laser Desorption/Ionization Time-of-Flight Mass Spectrometry. *Rapid Commun. Mass Spectrom.* **1999**, *13*, 508–515. [CrossRef]
111. Taylor, R.T.; Puapaiboon, U. Polyurethane Dendrimers via Curtius Reaction. *Tetrahedron Lett.* **1998**, *39*, 8005–8008. [CrossRef]
112. Poudel, D.P.; Taylor, R.T. A Model for Late-Stage Modification of Polyurethane Dendrimers Using Thiol—Ene Click Chemistry. *ACS Omega* **2021**, *6*, 12375–12381. [CrossRef]
113. Hou, X.; Butz, J.; Chen, J.; Wang, Z.D.; Zhao, J.X.; Shiu, T.; Chu, Q.R. Low Molecular Weight Organogelators Derived from Threefold Symmetric Tricarbamates. *Tetrahedron Lett.* **2017**, *58*, 101–105. [CrossRef]